

Obtaining and characterization of bioplastics based on potato starch, aloe, and graphene

Mercedes Puca Pacheco^{1*} , Oscar Rafael Tinoco Gómez² , Gonzalo Canché Escamilla³ ,
Santiago Duarte Aranda³  and María Guadalupe Neira Velázquez⁴ 

¹*Facultad de Ingeniería, Carrera de Ingeniería Industrial y Comercial, Universidad San Ignacio de Loyola, Lima, Perú*

²*Facultad de Ingeniería Industrial, Universidad Nacional Mayor de San Marcos, Lima, Perú*

³*Unidad de Materiales, Centro de Investigación Científica de Yucatán A.C., Yucatán, México*

⁴*Centro de investigación en Química Aplicada, Coahuila, México*

*mpucap@gmail.com

Abstract

Currently there is a great trend towards cleaner, more sustainable and green production, based on a circular economy. Therefore, in the present work the study of the effect of the concentration of potato starch, aloe vera and graphene on the mechanical properties, water vapor permeability, biodegradability and structural properties of bioplastics is reported. These bioplastics could replace conventional synthetic plastics that currently produce high environmental pollution. According to the statistical analysis of a 2³ factorial design, a biodegradable bioplastic with improved mechanical properties was obtained, with a high maximum stress of 2.49 ± 0.28 MPa at high concentration levels of starch, aloe vera and graphene (10% w/w starch, 24% w/w of aloe and 0.045% w/w of graphene). A minimum value of permeance and permeability to water vapor of 5.35 kg/h.kPa.m² and 0.001839 kg/h.kPa.m, respectively, was found at a graphene concentration of 0.005%; aloe concentration, 24%; and starch concentration, 10%.

Keywords: *graphene, bioplastic, biodegradable, mechanical properties, starch.*

How to cite: Puca Pacheco, M., Tinoco Gómez, O. R., Canché Escamilla, G., Duarte Aranda, S., & Neira Velázquez, M. G. (2022). Obtaining and characterization of bioplastics based on potato starch, aloe, and graphene. *Polímeros: Ciência e Tecnologia*, 32(4), e2022037. <https://doi.org/10.1590/0104-1428.20220084>

1. Introduction

Currently, interest has arisen in developing new materials to replace synthetic polymers that pollute the environment^[1]. To date, more than 8 billion tons of plastics have been produced in the last 70 years and an increase in non-biodegradable plastic waste is expected to exceed 25 billion metric tons by 2050^[2,3]. The waste produced causes very severe damage to the environment and biodiversity^[4,5]; since they contaminate the oceans by 85% and are even ingested by living organisms causing damage and death^[6,7].

Currently, the main strategy of the plastic industries is to adopt a circular economy instead of a linear economy. The circular economy consists of zero-waste manufacturing, which allows conventional plastic products to be remanufactured, reused, and recycled at the end of their useful life^[8,9]. Given this situation, biodegradable biopolymers can put an end to the problem of environmental pollution, since after their useful life, they degrade and are transformed into biomass again without harmful effects on the environment^[10,11].

The advantage of using biopolymers is that they do not pollute the environment, they are chemically versatile, sustainable, biocompatible, biodegradable, non-toxic,

renewable, not intrinsically functional and ecological^[12]. However, there is a need to improve the mechanical properties, transport properties (vapor and gas permeability), and poor processability among others. For this reason, there are other studies on the incorporation of cellulose nanoparticles, zinc, magnesium, copper and gold nanoparticles to obtain polymeric nanocomposites with better thermal and mechanical properties and biodegradability^[13,14].

Starch is the second most abundant carbohydrate in the biosphere after cellulose. In this work, Yungay potato starch was selected, due to its performance, processability and costs, which are the greatest challenges for the production of biodegradable polymers to be effective and fulfill the functions required during their useful life and final disposition of the product. Aloe vera gel has been used for the formation of the bioplastic since it is rich in mucilage, which is the source of polysaccharides containing galacturonic, glucuronic, and sugar-linked acids as glucose, galactose and arabinose; and phenolic compounds with great antioxidant power and act as an antibacterial agent in films^[15]. Aloe vera improves compatibility between starch and glycerin, preventing phase separation^[16].

On the other hand, graphene is a two-dimensional (2D) carbon nanostructure, with sp^2 hybridization, which was discovered by Geim and Novoselov^[17], they used scotch tape to peel graphene sheets from graphite. The important characteristics of graphene are its high thermal conductivity^[18], Young's modulus of 1 Terapascal, being 100 times stronger than steel and 6 times lighter than steel, also present good thermal and optical properties^[19], among other, for which it has created interest to be used in energy storage materials^[20], drug delivery systems^[21], biosensors^[22], polymeric compounds^[23], and in other areas.

In the present research work, a biodegradable bioplastic material based on yungay potato starch, aloe vera gel and graphene with better physicochemical and mechanical properties has been obtained at laboratory level, to be considered as an alternative material to synthetic plastics.

2. Experimental

2.1 Materials

For the synthesis of graphene, graphite from Sigma-Aldrich was used. Sulfuric acid at 98% w/w, potassium permanganate, concentrated hydrochloric acid at 36.5% w/w and ascorbic acid were also used and were acquired from Merck (Peru). Triple distilled, deionized and filtered water was used. Yungay potato tubers (*Solanum tuberosum*) from the department of Huánuco in Peru were used. Aloe vera (*barbadensis* Miller) from Lima was used. Venturo brand vinegar and glycerin acquired from Laboratory Alkofarma EIRL were used.

2.2 Method

2.2.1 Potato starch production process

The extraction of the starch was carried out at the laboratory level by means of a manual process. For this, the Yungay potato was harvested, washed and peeled, after which they were chopped into approximately 3 cm sizes and blended with cold boiled water in a proportion of 1: 1 to facilitate starch extraction. Then the starch was decanted and the supernatant liquid was then removed. The starch obtained was dried at 50 °C for 15 hours. Finally, the starch was pulverized and stored at a temperature of 20 °C^[24]. Thus, starch granules of 5 to 10 microns were obtained.

2.2.2 Obtaining the aloe vera gel

To obtain the aloe vera gel, the aloe leaves collected were washed to remove all impurities. They were then placed for 2 days in a bucket containing drinking water to remove the iodine. Then the bark was separated, to only keep the pulp (aloe vera). The separated pulp was chopped and subsequently liquefied for 5 minutes to obtain a good homogeneity.

2.2.3 Production of graphene by the modified Hummer method

The following procedure was used to obtain graphene: 0.5 g of graphite was weighed and poured into a 250 mL erlenmeyer flask, and then the flask, was placed in an ice bath, then 23 mL of concentrated sulfuric acid was slowly added, keeping the solution at a temperature below 20 °C and stirring for 4 hrs. Then 3 g of solid $KMnO_4$ were added

slowly and the stirring was maintained for 1 hour more in an ice bath. The solution was then heated to 35 °C, removing it from the ice bath, and keeping it under stirring for 1 hour more. Next, 45 mL of distilled water was added and then heated at 95 °C; keeping it under stirring for 2 hours. Then 10 mL of 30% hydrogen peroxide solution was added, and it was stirred for 1 hour more. Then 200 mL of a 5% m/v ascorbic acid solution was added to achieve the reduction of the graphene oxide and the solution was kept under stirring for 2 hours. In this stage, topological defects and vacancies produced during the elimination of functional groups can be created^[25]. Then, the graphene obtained was washed with distilled water and finally dried at 50 °C for 2 days.

2.2.4 Preparation of bioplastic films

For the preparation, potato starch was poured into the water, heated to 40 °C, and mixed for 10 minutes. Then 7 g of vinegar (5% w/v acetic acid) was added and stirred for 15 minutes to produce acid hydrolysis of starch and to remove amylopectin branches. Aloe vera gel was added and after 10 minutes of stirring, graphene (previously sonicated in 30 mL of distilled water for 30 minutes) was also added, and agitation was continued for another 15 minutes. Then 5 g of glycerin was added to provide flexibility to the bioplastic and the mixture was stirred for 10 minutes. The solution was heated between 60 °C and 70 °C and stirred for approximately 5 minutes until the mixture acquired a certain viscosity at the gelatinization temperature and then was poured into a 20 × 20 cm glass mold. Finally, the viscous mixture was dried in an oven at 60 °C for 10 hours. The amounts of starch, aloe vera and graphene used in the preparation of the films, were according to Table 1.

2.2.5 Experimental design

To evaluate the effect of the concentrations of Yungay potato starch, aloe vera gel, and graphene on the mechanical properties, and biodegradability of the films, an experimental design was proposed through a factorial design 2³ with three factors: the starch concentration (%w/w), the aloe concentration (%w/w) and the graphene concentration (%w/w), of two levels for each factor: high level (+) and low level (-) as shown in Table 1. A 2³ design was chosen since it allows estimating the effects of the independent variables and the combination of them, on the response variables with fewer experiments, it is cheaper and with the same precision than studying them separately^[26]. The range of graphene

Table 1. Factorial design 2³.

Experimental Run	Notation	[starch] % w/w	[aloe gel] % w/w	[Graphene] % w/w
	[starch] [aloe] [graphene]			
F1G	(+)(+)(+)	10	24	0.045
F2G	(-)(-)(-)	6	20	0.005
F3G	(+)(+)(-)	10	24	0.005
F4G	(+)(-)(+)	10	20	0.045
F5G	(-)(+)(-)	6	24	0.005
F6G	(-)(-)(+)	6	20	0.045
F7G	(+)(-)(-)	10	20	0.005
F8G	(-)(+)(+)	6	24	0.045

concentration was considered from 0.005 to 0.045%w/w since at graphene concentrations above 0.045%w/w formed brittle films and were not homogeneous.

In each run, the glycerin concentration was maintained at 5% w/w, vinegar concentration at 7% w/w and the rest distilled water was used until completing 100% in the formulation.

2.3 Characterization of materials and starch films

For the structural characterization, a Nicolet model protege 8700 equipment with an ATR accessory and ZnSe crystal was used, making 6 scans from 4000 to 650 cm^{-1} , and a resolution of 4 cm^{-1} .

For the film's biodegradability study, aerobic biodegradation was performed, which produces the complete oxidation of the bioplastic. To do this, they were measured by placing the films inside farmland prepared to be degraded by the natural action of microorganisms, decomposing into carbon dioxide, water and/or methane and biomass, and the bioplastic films were weighed every 7 days for 1 month. To calculate weight loss, a test was carried out for a period of a month. The following Equation 1 was used:

$$\text{Weight Loss \%} = \frac{\text{Initial Dry Weight (g)} - \text{Final Dry Weight (g)}}{\text{Initial Dry Weight (g)}} * 100 \quad (1)$$

In this work, the water solubility of the bioplastic was determined according to the methodology proposed by Gontard et al.^[27] The bioplastics were cut in a circular shape with a diameter of 2 cm, weighed, and then immersed in 50 mL of distilled water contained in glass beakers. The samples were kept in water and stirred for 24 hours at 25 °C. The samples were dried (105 ± 2 °C for 24 hours) in a drying oven, and then the dry weight of the bioplastic that was not solubilized was determined. The solubility is expressed according to Equation 2:

$$\% \text{ Solubility} = \left(1 - \frac{(PI - PF)}{PI} \right) * 100 \quad (2)$$

where:

PI: Initial weight of bioplastic (g);

PF: Final weight of dry bioplastic that was not solubilized in water (g).

The morphology analysis of the cross section of the bioplastics was observed using a JEOL 6360LV SEM scanning electron microscope operated at 20 kV.

To carry out the mechanical tests of the films with an average thickness of 324 microns, the samples were conditioned at a temperature of 25 °C and relative humidity (RH) of 66 ± 4% RH for 24 hours prior to the mechanical tests. The tests were carried out on a Shimadzu AGS-X universal machine with a 100 N load cell. The speed of the test was 3 mm/min, according to the ASTM D 882 standard.

For the determination of the water vapor transmission (WVT) and the permeance in the starch/aloe vera/graphene films, the standard ASTM E96/E96M-14: Standard Test Method for Water Vapor Transmission of Materials was used, using the desiccant method or dry cup method. The water

vapor transmission (WTV) and water vapor permeance values were calculated from the following expressions:

Water Vapor Transmission Rate, WVT:

$$WVT = \frac{G/t}{A} \quad (3)$$

where:

G = weight change, in grams (from linear graph G/t);

t = time, hours;

A = exposure area, m^2 (canopy area: 0.0025 m^2).

Permeance:

$$\text{Permeance} = \frac{WVT}{\Delta P} \quad (4)$$

where:

$\Delta p = S (R1 - R2)$,

S = mmHg (Absolute saturated vapor pressure at a temperature of 23 °C., 21.068 mmHg) *

R1 = Relative humidity of the crown, that is, 1

R2 = Relative humidity at normal laboratory conditions (0.5)

* Value reported per ASTM D1653-1 standard (Standard Test Methods for Water Vapor Transmission of Organic Coating Films).

Permeability:

$$\text{Permeability} = \text{Permeance} * \text{Thickness} \quad (5)$$

The bioplastic films evaluated had an average thickness of 0.3437 mm.

3. Results and Discussion

3.1 Structural characterization of starch and aloe vera.

Table 2 shows the yield and composition chemical of Yungay potato starch. A starch yield of 8.13% was obtained with respect to the dry weight of the potato. The content of amylose (linear polymer) and amylopectin (branched polymer) was 25.67% and 74.32% respectively.

Aloe vera leaves are made up of a gel and a bark that represent 60.2 and 39.8% of the weight of the fresh leaf, respectively. The aloe vera gel is mainly made up of water (99.1%) and the 0.9% remaining are mucilage and other carbohydrates^[31,32].

Table 2. Characterization of Yungay potato starch.

Feature	Yungay potato starch	Method
Extraction Performance	8.13 ± 1.22	Gravimetric method
Humidity (%)	13.42 ± 1.87	AOAC 950.46 ^[28] .
Amylose (%)	25.67 ± 6.45	Hoover and Ratnayake ^[29] .
Amylopectin (%)	74.32 ± 6.45	Hoover and Ratnayake ^[29] .
Gelatinization temperature (%)	64.50 ± 1.98	Grace ^[30] .
Total protein (%)	1.03 ± 0.15	AOAC 984.13 ^[28] .

The infrared spectrum of dry aloe vera gel (Figure 1) shows the functional groups of these compounds. The broad absorption band centered at 3424 cm^{-1} is due to the stretching of -OH groups, a characteristic of carbohydrate monomers, such as mannose and uronic acid^[33,34]. The absorption band at 2922 cm^{-1} can be assigned to symmetric and asymmetric C-H stretching of aliphatic -CH and -CH₂ groups. The absorption band at 1743 cm^{-1} is a characteristic of C=O stretching, which indicates the presence of carbonyl groups in aloe vera samples, which is not seen in the infrared spectrum of starch and allows them to be differentiated. The absorption reaches its maximum point at 1634 and 1418 cm^{-1} , these signals are associated, respectively, with the asymmetric and symmetric stretching of carboxylate compounds -COO- in aloe vera. The absorption peak at 870 cm^{-1} is due to out-of-plane C-H deformation of the carbohydrate monomers. These absorption peaks indicate the presence of mannose and uronic acid, as well as their carbohydrate polymers^[35,36].

3.2 Structural analysis of graphene

Figure 2 shows the infrared spectrum of graphene synthesized by the modified Hummer method, showing a band around 1600 cm^{-1} , which corresponds to the stretching vibration of the C=C bond, another peak located around 1100 cm^{-1} due to the vibration of the ether group (C-O-C), and also other peaks associated to the stretching and bending

vibration of the O-H bond around $3000 - 3500\text{ cm}^{-1}$ and at 1400 cm^{-1} , are shown^[37].

3.3 Structural characterization of bioplastic films

Figure 3 shows the FTIR spectra corresponding to the samples with the high level (F1G) and the lower level (F2G) of the components (see the factorial design in Table 1). In the region from 400 to 1250 cm^{-1} considered the fingerprint region^[38], there were four characteristic peaks in the spectra between 925 and 1150 cm^{-1} , which are attributed to the stretching of the CO bond^[39]. The peak located at 1467 cm^{-1} is assigned to the bending of the CH₂ group and the broad peak between 2900 and 2950 cm^{-1} , is characteristic of the C-H stretches associated with the glucopyranose ring^[40]. The broad peak between 3000 and 3700 cm^{-1} is due to the hydrogen bonding of the hydroxyl groups that contributes to the stretching vibrations associated with the inter and intramolecular free bonding of the hydroxyl group, and this group being a characteristic of the structure of the starch^[41].

3.4 Biodegradability tests of bioplastic films

Table 3 shows the results of the % biodegradability after 30 days of exposure, which are between 75.61 and 94.37% . Graphene is chemically inert since it does not corrode or degrade in the presence of atmospheric agents such as light, humidity and pH^[42,43], so the film decomposition is mainly

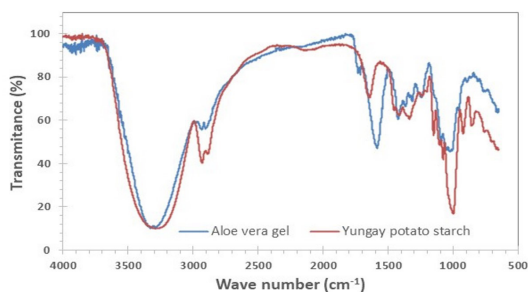


Figure 1. Infrared spectra of dried aloe vera and Yungay potato starch samples.

Table 3. Biodegradability properties of bioplastic films at 30 days of evaluation and solubility in water of bioplastic films at 24 hours.

Sample	Code	Biodegradability (%)	Solubility in Water (%)
F1G	(+)(+)(+)	77.52	41.00 ± 0.11
F2G	(-)(-)(-)	94.37	57.05 ± 0.31
F3G	(+)(+)(-)	77.04	37.02 ± 0.41
F4G	(+)(-)(+)	79.48	53.81 ± 0.51
F5G	(-)(+)(-)	88.62	49.10 ± 0.31
F6G	(-)(-)(+)	80.85	59.93 ± 0.67
F7G	(+)(-)(-)	79.07	45.79 ± 0.44
F8G	(-)(+)(+)	75.61	54.40 ± 0.06

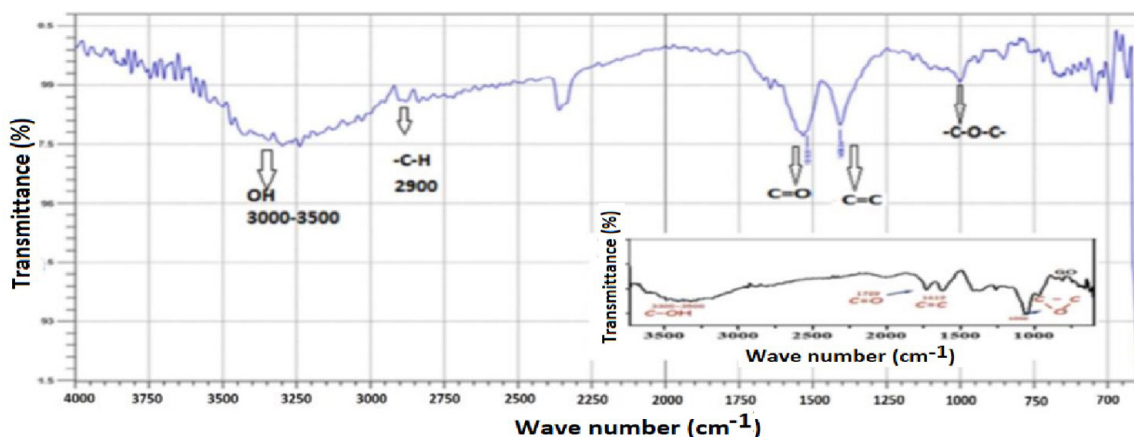


Figure 2. The infrared spectrum of graphene, obtained by the modified Hummer method^[37].

due to organic matter such as starch and organic compounds present in aloe gel. The degradation capacity of bioplastics is due to the hydrophilic nature of starch, which is increased by containing glycerin, which produces greater adsorption of water, which favors the cultivation of starch-degrading bacteria and fungi. The biodegradation is catalyzed by the action of enzymes that break the bonds between the anhydroglucose molecules of the starch chains^[44].

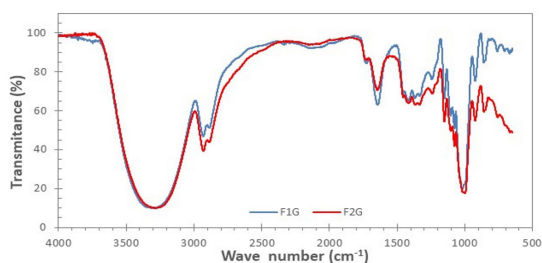


Figure 3. Infrared spectra of bioplastic samples with the higher level (F1G) and the lower level (F2G) of the components (potato starch, aloe vera, and graphene).

Table 3 shows that the bioplastic films have a solubility in water between 41.00 ± 0.11 and $59.93 \pm 0.67\%$, which can be attributed to the glycerin present in the film. The remotion of compounds soluble in water, such as glycerin and oligomers, increases because water has a high affinity with the starch matrix which results in the acceleration of the diffusion of water through the polymeric film. It was found that increasing the content of graphene in the formulation, results in a higher solubility of the films.

3.5 Morphological study

Figure 4 shows the images obtained by SEM of the cryogenic fracture zone of the graphene-reinforced films with a higher concentration of graphene (0.045% w/w) at different magnifications. It can be observed that all samples show the presence of several stacked graphene sheets with a dense, wrinkled and folded morphology (indicated by the arrow in Figure 4b) and this is more notorious when the high level of starch was used in the films (F1G and F4G). These films show the presence of starch granules in one face of the films, and the films can be appreciated in the cross section of an irregular fracture of the film.

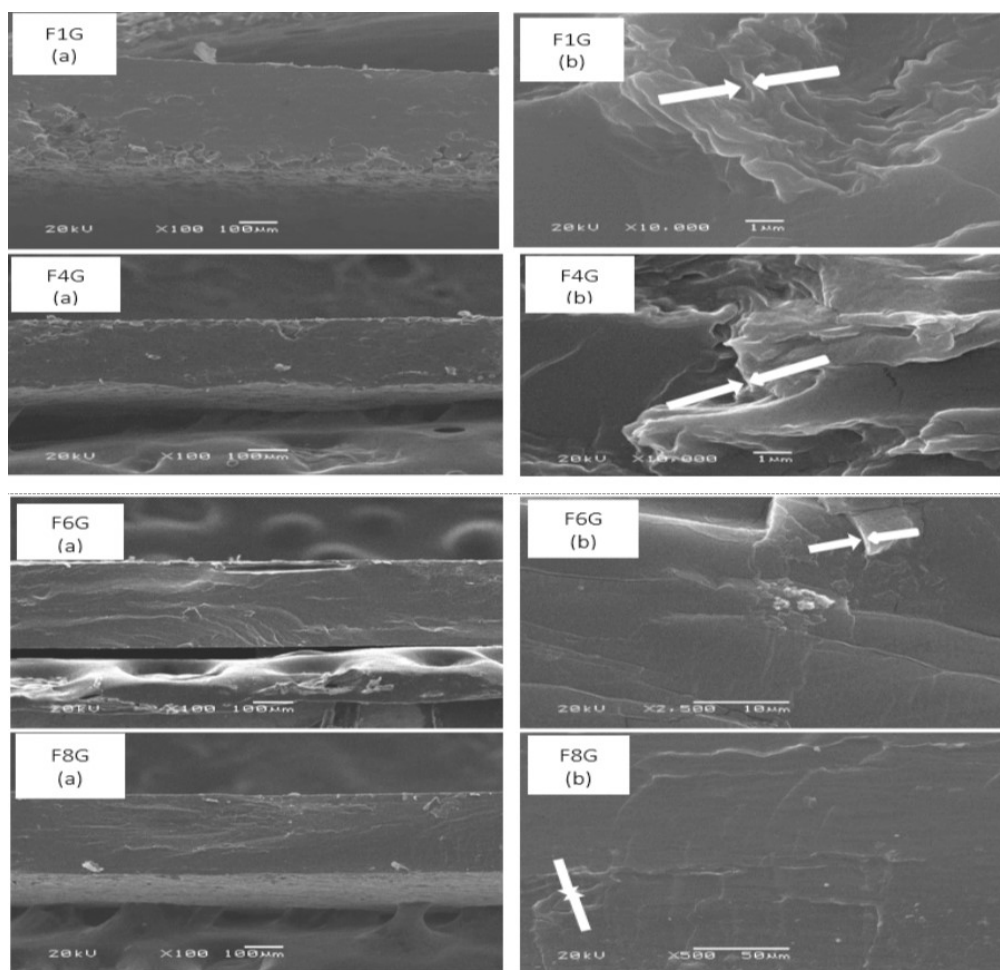


Figure 4. Images obtained by SEM of the cross section (a) and of the surface of the cross section at higher amplitude (b) of bioplastic films with a graphene concentration of 0.045% w/w.

3.6 Mechanical properties

According to Table 4, it is important to point out that the maximum stress was higher in the high level of starch, aloe and graphene concentration compared with the low level.

According to the results shown in Table 4, the maximum stress was between 2.49 ± 0.28 and 1.09 ± 0.10 MPa and the % elongation at break was between 63.67 ± 6.26 and $29.06 \pm 2.15\%$.

A decrease in Maximum stress from 1.93 MPa to 1.36 MPa and an increase in % elongation at break from 29.06 to 63.67% was observed when the weight ratio of glycerin and starch was increased from 5:10 to 5:6 in run F4G and F6G respectively (see Table 1). Similar behavior to that reported by Meneses et al.^[45] who pointed out that the increase in the dose of glycerin reduces the intermolecular forces, such as internal hydrogen bonds, causing the bioplastic to be flexible and less resistant, increasing the intermolecular spaces, and avoiding cracks in the bioplastic during its manipulation and storage.

3.6.1 Statistical analysis of the results.

For the ANOVA analysis of the results obtained the Minitab Statistical Software Version 21.1. 0 was used. Table 5 shows the analysis of variance for maximum stress and elongation at break (%). According to the study of the principal effect, a significant effect of the starch concentration on maximum stress, and strain at break was obtained with a p-value of 0.0000. Also, there was a significant effect of aloe concentration on maximum stress, and elongation at break (%) with a p-value of 0.0024 and 0.0139 respectively. Finally, there was a significant effect of graphene concentration on maximum stress, and elongation at break (%) with a p-value of 0.0005 and 0.0141 respectively.

According to the main effects, a direct effect of the concentration of starch, aloe and graphene on the maximum resistance was found. However, an inverse effect of starch concentration on elongation at break(%) and a direct effect of aloe and graphene concentration on elongation at break were found.

3.7 Permeability

Table 6 show the result of permeance and permeability of bioplastic film for design 2³ with two central points.

3.7.1 Statistical analysis of the results.

Table 7 shows the analysis of variance of the permeability results, which was obtained using the statistical software Minitab 21.1.0 and it was found that the concentration of starch and the concentration of graphene had a significant effect with p values of 0.029 and 0.044 (p-value < 0.05). However, the concentration of aloe had no significant effect. It was shown that the permeability to water vapor depends not only on the concentration of graphene (filler) and the concentration of starch, but there is also an interaction between the concentration of starch and graphene, which determines the dispersion, the affinity of the permeant gas molecule - membrane and the morphology of the nanoparticle.

Table 4. Mechanical characterization of bioplastic films based on starch, graphene, and aloe vera gel.

Sample	Code	Maximum stress (MPa)	Elongation at break (%)
F1G	(+)(+)(+)	2.49 ± 0.28	32.51 ± 6.92
F2G	(-)(-)(-)	1.09 ± 0.10	33.60 ± 5.89
F3G	(+)(+)(-)	1.96 ± 0.10	43.26 ± 2.17
F4G	(+)(-)(+)	1.93 ± 0.40	29.06 ± 2.15
F5G	(-)(+)(-)	1.19 ± 0.07	49.49 ± 2.28
F6G	(-)(-)(+)	1.36 ± 0.03	63.67 ± 6.26
F7G	(+)(-)(-)	1.36 ± 0.04	30.99 ± 3.93
F8G	(-)(+)(+)	1.36 ± 0.05	55.14 ± 5.34

Table 5. Analysis of Variance for maximum stress, and elongation at break.

Interactions and effects	P-Value	P-Value
	Maximum stress (MPa)	Elongation at break (%)
A: Starch concentration (%)	0.0000*	0.0000*
B: Aloe vera concentration (%)	0.0024*	0.0139*
C: Graphene concentration (%)	0.0005*	0.0141*
AB	0.0579	0.3341
AC	0.3419	0.0000*
BC	0.6800	0.0000*

*Significance value (P<0.05).

Table 6. Permeance and permeability of bioplastic films based on starch, aloe and graphene^[46]

Sample	Code	WVT (g/h.m ²)	Permeance (kg/Pa.h.m ²)	Permeability (kg/Pa.h.m)
F1G	(+)(+)(+)	7.81	5.56	0.001911
F2G	(-)(-)(-)	9.30	6.62	0.002275
F3G	(+)(+)(-)	7.52	5.35	0.001839
F4G	(+)(-)(+)	8.17	5.81	0.001997
F5G	(-)(+)(-)	11.13	7.92	0.002722
F6G	(-)(-)(+)	22.69	16.10	0.005534
F7G	(+)(-)(-)	12.26	8.73	0.003000
F8G	(-)(+)(+)	18.50	13.17	0.004527
I1	(0)(0)(0)	24.03	17.10	0.005878
I2	(0)(0)(0)	23.42	16.68	0.005733

Table 7. Analysis of variance of the permeability of bioplastic films.

Interactions and Effects	p-value
Main effects	
A: Starch concentration (%)	0.029*
B: Aloe vera concentration (%)	0.101
C: Graphene concentration (%)	0.044*
AB	0.253
AC	0.031*
BC	0.415
ABC:	0.072

*p-value < 0.05.

4. Conclusions

A biodegradable bioplastic material based on starch, aloe vera, and graphene using an experimental design 2³ with

improved mechanical properties was obtained, with a high maximum stress of 2.49 ± 0.28 MPa at high levels of starch, aloe and graphene concentration (10%w/w starch, 24%w/w aloe and 0.045%w/w graphene).

Therefore, the use of aloe, starch and graphene is convenient to obtain better mechanical properties. Likewise, using graphene and aloe vera, maximum stress is improved, and the strain at break is increased, that is, it gives flexibility to the bioplastic.

A minimum permeance and permeability value of 5.35 kg/h.kPa.m² and 0.001839 kg/h.kPa.m, respectively, was found at a graphene concentration of 0,005%; aloe concentration, 24%; and starch concentration, 10%.

For future studies, the antimicrobial properties in the bioplastic film will be measured. Also, other reinforcing materials will be used, such as nanocellulose fibers, in order to further improve the mechanical properties.

5. Author's Contribution

- **Conceptualization** – NA.
- **Data curation** – NA.
- **Formal analysis** – Mercedes Puca Pacheco; Oscar Tinoco Gómez.
- **Funding acquisition** – NA.
- **Investigation** – Mercedes Puca Pacheco.
- **Methodology** – Mercedes Puca Pacheco.
- **Project administration** – NA
- **Resources** – Mercedes Puca Pacheco; María Guadalupe Neira Velázquez; Gonzalo Canché Escamilla; Santiago Duarte Aranda; Manuel Aguilar Vega.
- **Software** – NA.
- **Supervision** – NA.
- **Validation** – NA.
- **Visualization** – NA.
- **Writing – original draft** – Mercedes Puca Pacheco.
- **Writing – review & editing** – Mercedes Puca Pacheco; Gonzalo Canché Escamilla; María Guadalupe Neira Velázquez.

6. Acknowledgements

The authors thank María Isabel Loría Bastarrachea (CICY) for her support in running the water vapor permeability tests.

7. References

1. Mohanty, A. M., Misra, M., & Drzal, L. T. (Eds.). (2005). *Natural fibers, biopolymers, and biocomposites*. USA: CRC Press. <http://dx.doi.org/10.1201/9780203508206>.
2. Kartik, A., Akhil, D., Lakshmi, D., Gopinath, K. P., Arun, J., Sivaramkrishnan, R., & Pugazhendhi, A. (2021). A critical review on production of biopolymers from algae biomass and their applications. *Bioresource Technology*, 329, 124868. <http://dx.doi.org/10.1016/j.biortech.2021.124868>. PMID:33707076.
3. Khalid, M. Y., Arif, Z. U., Ahmed, W., & Arshad, H. (2022). Recent trends in recycling and reusing techniques of different plastic polymers and their composite materials. *Sustainable Materials and Technologies*, 31, e00382. <http://dx.doi.org/10.1016/j.susmat.2021.e00382>.
4. Khalid, M. Y., & Arif, Z. U. (2022). Novel biopolymer-based sustainable composites for food packaging applications: a narrative review. *Food Packaging and Shelf Life*, 33, 100892. <http://dx.doi.org/10.1016/j.foodpack.2022.100892>.
5. Haghghi, H., Gullo, M., La China, S., Pfeifer, F., Siesler, H. W., Licciardello, F., & Pulvirenti, A. (2021). Characterization of bio-nanocomposite films based on gelatin/polyvinyl alcohol blend reinforced with bacterial cellulose nanowhiskers for food packaging applications. *Food Hydrocolloids*, 113, 106454. <http://dx.doi.org/10.1016/j.foodhyd.2020.106454>.
6. Barati, Z., Latif, S., & Müller, J. (2019). Enzymatic hydrolysis of cassava peels as potential pre-treatment for peeling of cassava tubers. *Biocatalysis and Agricultural Biotechnology*, 20, 101247. <http://dx.doi.org/10.1016/j.bcab.2019.101247>.
7. Morales, A., Labidi, J., Gullón, P., & Astray, G. (2021). Synthesis of advanced biobased green materials from renewable biopolymers. *Current Opinion in Green and Sustainable Chemistry*, 29, 100436. <http://dx.doi.org/10.1016/j.cogsc.2020.100436>.
8. Gorak, P., Postawa, P., Trusilewicz, L. N., & Kalwik, A. (2021). Cementitious eco-composites and their physicochemical/mechanical properties in Portland cement-based mortars with a lightweight aggregate manufactured by upcycling waste by products. *Journal of Cleaner Production*, 289, 125156. <http://dx.doi.org/10.1016/j.jclepro.2020.125156>.
9. Berger, F., Gauvin, F., & Brouwers, H. J. H. (2020). The recycling potential of wood waste into wood-wool/cement composite. *Construction & Building Materials*, 260, 119786. <http://dx.doi.org/10.1016/j.conbuildmat.2020.119786>.
10. Marczak, D., Lejcuś, K., Grzybowska-Pietras, J., Biniś, W., Lejcuś, I., & Misiewicz, J. (2020). Biodegradation of sustainable nonwovens used in water absorbing geocomposites supporting plants vegetation. *Sustainable Materials and Technologies*, 26, e00235. <http://dx.doi.org/10.1016/j.susmat.2020.e00235>.
11. Chan, C. M., Vandi, L.-J., Pratt, S., Halley, P., Richardson, D., Werker, A., & Laycock, B. (2019). Insights into the biodegradation of PHA/wood composites: micro- and macroscopic changes. *Sustainable Materials and Technologies*, 21, e00099. <http://dx.doi.org/10.1016/j.susmat.2019.e00099>.
12. Arif, Z. U., Khalid, M. Y., Sheikh, M. F., Zolfagharian, A., & Bodaghi, M. (2022). Biopolymeric sustainable materials and their emerging applications. *Journal of Environmental Chemical Engineering*, 10(4), 108159. <http://dx.doi.org/10.1016/j.jece.2022.108159>.
13. Liu, Y., Ahmed, S., Sameen, D. E., Wang, Y., Lu, R., Dai, J., Li, S., & Qin, W. (2021). A review of cellulose and its derivatives in biopolymer-based for food packaging application. *Trends in Food Science & Technology*, 112, 532-546. <http://dx.doi.org/10.1016/j.tifs.2021.04.016>.
14. Sobhan, A., Muthukumarappan, K., & Wei, L. (2021). Biosensors and biopolymer-based nanocomposites for smart food packaging: challenges and opportunities. *Food Packaging and Shelf Life*, 30, 100745. <http://dx.doi.org/10.1016/j.foodpack.2021.100745>.
15. Lefsih, K., Iboukhoulef, L., Petit, E., Benouat, H., Pierre, G., & Delattre, C. (2018). Anti-Inflammatory and Antioxidant Effect of a D-galactose-rich Polysaccharide Extracted From Aloe vera Leaves. *Advances in Applied Chemistry and Biochemistry*, 1(1), 18-26. <http://dx.doi.org/10.33513/ACBC/1801-03>.
16. Kakroodi, A. R., Cheng, S., Sain, M., & Asiri, A. (2014). Mechanical, thermal, and morphological properties of nanocomposites based on polyvinyl alcohol and cellulose nanofiber from Aloe vera rind. *Journal of Nanomaterials*, 903498, 1-7. <http://dx.doi.org/10.1155/2014/903498>.

17. Geim, A. K., & Novoselov, K. S. (2007). The rise of graphene. *Nature Materials*, 6(3), 183-191. <http://dx.doi.org/10.1038/nmat1849>. PMID:17330084.
18. Balandin, A. A., Ghosh, S., Bao, W., Calizo, I., Teweldebrhan, D., Miao, F., & Lau, C. N. (2008). Superior thermal conductivity of single-layer graphene. *Nano Letters*, 8(3), 902-907. <http://dx.doi.org/10.1021/nl0731872>. PMID:18284217.
19. Lonkar, S. P., Deshmukh, Y. S., & Abdala, A. A. (2015). Recent advances in chemical modifications of graphene. *Nano Research*, 8(4), 1039-1074. <http://dx.doi.org/10.1007/s12274-014-0622-9>.
20. Zhang, J., Zhao, F., Zhang, Z., Chen, N., & Qu, L. T. (2013). Dimension-tailored functional graphene structures for energy conversion and storage. *Nanoscale*, 5(8), 3112-3126. <http://dx.doi.org/10.1039/c3nr00011g>. PMID:23467313.
21. Liu, J., Cui, L., & Losic, D. (2013). Graphene and graphene oxide as a new nanocarriers for drug delivery applications. *Acta Biomaterialia*, 9(12), 9243-9257. <http://dx.doi.org/10.1016/j.actbio.2013.08.016>. PMID:23958782.
22. Kuila, T., Bose, S., Khanra, P., Mishra, A. K., Kim, N. H., & Lee, J. H. (2011). Recent advances in graphene based biosensors. *Biosensors & Bioelectronics*, 26(12), 4637-4648. <http://dx.doi.org/10.1016/j.bios.2011.05.039>. PMID:21683572.
23. Du, J. H., & Cheng, H.-M. (2012). The fabrication, properties, and uses of graphene/polymer composites. *Macromolecular Chemistry and Physics*, 213(10-11), 1060-1077. <http://dx.doi.org/10.1002/macp.201200029>.
24. Avellán, A., Díaz, D., Mendoza, A., Zambrano, M., Zamora, Y., & Riera, M. A. (2019). Obtaining bioplastic from corn starch (*Zea mays L.*). *Revista Colón Ciencias, Tecnología y Negocios*, 7(1), 1-11. Retrieved in 2022, September 4, from <http://portal.amelica.org/ameli/jatsRepo/215/215974004/215974004.pdf>
25. Ramanathan, T., Abdala, A. A., Stankovich, S., Dikin, D. A., Herrera-Alonso, M., Piner, R. D., Adamson, D. H., Schniepp, H. C., Chen, X., Ruoff, R. S., Nguyen, S. T., Aksay, I. A., Prud'Homme, R. K., & Brinson, L. C. (2008). Functionalized graphene sheets for polymer nanocomposites. *Nature Nanotechnology*, 3(6), 327-331. <http://dx.doi.org/10.1038/nnano.2008.96>. PMID:18654541.
26. Montgomery, D. C. (2008). *Diseño y análisis de experimentos*. México: Limusa Wiley.
27. Gontard, N., Guilbert, S., & Cuq, J.-L. (1993). Water and glycerol as plasticizers affect mechanical and water vapor barrier properties of an edible wheat gluten film. *Journal of Food Science*, 58(1), 206-211. <http://dx.doi.org/10.1111/j.1365-2621.1993.tb03246.x>.
28. Association of Official Analytical Chemists – AOAC. (2005). *Official methods of analysis of the Association of Official Analytical Chemists*. USA: AOAC International.
29. Hoover, R., & Ratnayake, W. S. (2001). Determination of total amylose content of starch. *Current Protocols in Food Analytical Chemistry*, 00(1), E2.3.1-E2.3.5. <http://dx.doi.org/10.1002/0471142913.fae0203s00>.
30. Organización de las Naciones Unidas para la Agricultura y la Alimentación - FAO. *Elaboración de la yuca*. Italy: Organización de las Naciones Unidas para la Agricultura y la Alimentación – FAO.
31. Reynolds, T., editor (2004). *Aloes: The Genus Aloe. Medicinal and aromatic plants-industrial profiles*. USA: CRC Press LLC. <http://dx.doi.org/10.1201/9780203476345>.
32. Hamman, J. H. (2008). Composition and applications of Aloe vera leaf gel. *Molecules*, 13(8), 1599-1616. <http://dx.doi.org/10.3390/molecules13081599>. PMID:18794775.
33. Nejatizadeh-Barandozi, F., & Enferadi, S. T. (2012). FT-IR study of the polysaccharides isolated from the skin juice, gel juice, and flower of Aloe vera tissues affected by fertilizer treatment. *Organic and Medicinal Chemistry Letters*, 2(1), 33. <http://dx.doi.org/10.1186/2191-2858-2-33>. PMID:23095284.
34. Gentilini, R., Bozzini, S., Munarin, F., Petrini, P., Visai, L., & Tanzi, M. C. (2014). Pectins from Aloe Vera: extraction and production of gels for regenerative medicine. *Journal of Applied Polymer Science*, 131(2), n/a. <http://dx.doi.org/10.1002/app.39760>.
35. Rodríguez-González, V.-M., Femenia, A., González-Laredo, R. F., Rocha-Guzmán, N. E., Gallegos-Infante, J. A., Candelas-Cadillo, M. G., Ramírez-Baca, P., Simal, S., & Rosselló, C. (2011). Effects of pasteurización on bioactive polysaccharide acemannan and cell wall polymers from Aloe barbadensis Miller. *Carbohydrate Polymers*, 86(4), 1675-1683. <http://dx.doi.org/10.1016/j.carbpol.2011.06.084>.
36. Jithendra, P., Rajam, A. M., Kalaivani, T., Mandal, A. B., & Rose, C. (2013). Preparation and characterization of Aloe vera blended collagen-chitosan composite scaffold for tissue engineering applications. *ACS Applied Materials & Interfaces*, 5(15), 7291-7298. <http://dx.doi.org/10.1021/am401637c>. PMID:23838342.
37. Puca Pacheco, M., Tacuri Calanchi, E., Pantoja Cadillo, A., Neira Velázquez, M. G., & Canché Escamilla, G. (2017). Synthesis of polymer nanocomposites with graphene and their mechanical characterization. *Revista de la Sociedad Química del Perú*, 83(1), 65-77. <http://dx.doi.org/10.37761/rsqp.v83i1.104>.
38. Olsen, E. D. (1990). *Optical methods of analysis*. México: Editorial Reverté.
39. Goheen, S. M., & Wool, R. P. (1991). Degradation of polyethylene-starch blends in soil. *Journal of Applied Polymer Science*, 42(10), 2691-2701. <http://dx.doi.org/10.1002/app.1991.070421007>.
40. Mano, J. F., Koniarova, D., & Reis, R. L. (2003). Thermal properties of thermoplastic starch/synthetic polymer blends with potential biomedical applicability. *Journal of Materials Science. Materials in Medicine*, 14(2), 127-135. <http://dx.doi.org/10.1023/A:1022015712170>. PMID:15348484.
41. Fang, J. M., Fowler, P. A., Tomkinson, J., & Hill, C. A. S. (2002). The preparation and characterization of a series of chemically modified potato starches. *Carbohydrate Polymers*, 47(3), 245-252. [http://dx.doi.org/10.1016/S0144-8617\(01\)00187-4](http://dx.doi.org/10.1016/S0144-8617(01)00187-4).
42. Nan, H. Y., Ni, Z. H., Wang, J., Zafar, Z., Shi, Z. X., & Wang, Y. Y. (2013). The thermal stability of graphene in air investigated by Raman spectroscopy. *Journal of Raman Spectroscopy: JRS*, 44(7), 1018-1021. <http://dx.doi.org/10.1002/jrs.4312>.
43. Ohno, Y., Maehashi, K., Yamashiro, Y., & Matsumoto, K. (2009). Electrolyte gated graphene field-effect transistors for detecting ph and protein adsorption. *Nano Letters*, 9(9), 3318-3322. <http://dx.doi.org/10.1021/nl901596m>. PMID:19637913.
44. Myllärinen, P., Partanen, R., Seppälä, J., & Forssell, P. (2002). Effect of glycerol on the behavior of amylose and amylopectin films. *Carbohydrate Polymers*, 50(4), 355-361. [http://dx.doi.org/10.1016/S0144-8617\(02\)00042-5](http://dx.doi.org/10.1016/S0144-8617(02)00042-5).
45. Meneses, J., Corrales, C. M., & Valencia, M. (2013). Synthesis and characterization of a biodegradable polymer from cassava starch. *Revista EIA*, 4(8), 57-67. Retrieved in 2022, September 4, from <https://revistabme.eia.edu.co/index.php/reveia/article/view/185>
46. Puca Pacheco, M., Aguilar Vega, M., Canché Escamilla, G., & Neira Velázquez, M. G. (2022). Evaluation of thermal properties and permeability of bioplastic films based on starch, aloe vera and graphene. *Revista de la Sociedad Química del Perú*, 88(1), 63-77. <http://dx.doi.org/10.37761/rsqp.v88i1.376>.

Received: Sept. 04, 2022

Revised: Nov. 17, 2022

Accepted: Nov. 25, 2022